Dynamics of carving runs in alpine skiing. II.Centrifugal pendulum with a retractable leg.

Serguei S. Komissarov
Department of Applied Mathematics
The University of Leeds
Leeds, LS2 9JT, UK
e-mail: s.s.komissarov@leeds.ac.uk

Abstract

In this paper we present an advanced model of centrifugal pendulum where its length is allowed to vary during swinging. This modification accounts for flexion and extension of skier's legs when turning. We focus entirely on the case where the pendulum leg shortens near the vertical position, which corresponds to the most popular technique for the transition between carving turns in ski racing, and study the effect of this action on the kinematics and dynamics of these turns. In particular, we find that leg flexion on approach to the summit point is a very efficient way of preserving the contact between skis and snow. The up and down motion of the skier centre of mass can also have strong effect of the peak ground reaction force experienced by skiers, particularly at high inclination angles. Minimisation of this motion allows a noticeable reduction of this force and hence of the risk of injury. We make a detailed comparison between the model and the results of a field study of slalom turns and find a very good agreement. This suggests that the pendulum model is a useful mathematical tool for analysing the dynamics of skiing.

Keywords: alpine skiing, modelling, balance/stability, performance

Introduction

The skiing of expert skiers is characterised by smooth and rhythmic moves which are very reminiscent of a pendulum or metronome. This analogy invites mathematical modelling of skiing based on the pendulum action, which can be traced back to the pioneering work by Morawski (1973). They argued that a skier can be treated as pendulum's load and their skis as its pivot point. Such an inverted pendulum, with

its load located above its pivot, can be prevented from falling under the action of the gravity force, provided the pivot is allowed to slide horizontally under the action of a control force which pushes it in the direction to which the pendulum is leaning.

Recently we proposed a variant of this model, where the control force is replaced with the snow reaction force naturally emerging in carving turns (Komissarov, 2020). In perfect carving turns, the snow reaction force makes skis to move along quasi-circular arcs whose centre is located on the same side of the arc as the skier centre of mass (CM). Thus, the skis are forced to return back under the CM, like in the controlled inverted pendulum. On hard snow, the local curvature radius of carved ski tracks is fully determined by the ski sidecut radius R_{sc} (which is a fixed parameter of the skis) and the local ski tilt (or inclination) angle to the slope Ψ (Howe, 1983, page 101). Hence, given the skis speed, we can immediately find their acceleration.

The dynamics of such pendulum is easy to analyse in the accelerated frame of its pivot (skis), where the load is subjected to the gravity force, the leg reaction force, and the centrifugal force determined by the pendulum inclination. The gravity pushes the load towards the ground, the centrifugal force pushes it back to the vertical position and the leg reaction force controls the separation between the load and the pivot. We called such a pendulum centrifugal (Komissarov, 2020).

In addition to the vertical equilibrium of the traditional inverted pendulum, the centrifugal pendulum can have two more equilibria, one on each side, where the total torque due to the gravity and centrifugal force vanishes. These balanced (equilibrium) positions of the pendulum are inclined to the vertical by the angle

$$\Psi_{eq} = \arcsin\zeta\,, \tag{1}$$

where

$$\zeta = \frac{V^2}{gR_{sc}} \tag{2}$$

and V is the ski speed. Since skiing practitioners often describe balanced body position as an essential ingredient of advanced skiing, it may seem only natural to focus on the incline equilibria and the properties of corresponding carving turns. Theoretical analysis of such quasi-static turns has been carried out in several studies (e.g. Howe, 1983; Jentschura & Fahrbach, 2004; Komissarov, 2018). However, the inclined equilibria exist only when $\zeta < 1$ (the subcritical regime). This condition is equivalent to the upper limit $V < \sqrt{gR_{sc}}$ on the skier speed. Although this limit is quite high, the typical speeds of top ski racers are still higher (Komissarov, 2018, 2020), showing that skiing in balance is not the only option. Moreover, the inclined equilibria are unstable and hence impossible to sustain, unless an additional control force is introduced into the system (Komissarov, 2018, 2020).

Fortunately, it turns out that the model of centrifugal pendulum also allows oscillations about the vertical equilibrium (Komissarov, 2020). In the subcritical regime their amplitude is limited from above by Ψ_{eq}. In the supercritical regime ($\zeta > 1$) the amplitude is not limited, apart from the obvious limit $\Psi < 90^\circ$ set by the

presence of solid ground. In these solutions the pendulum is never in equilibrium, and the forces are never balanced. This finding shows that the force balance is actually not an inherent feature of ski turns and invites us to re-examine the way we see alpine skiing. In Komissarov (2020), we associated the oscillatory solutions with the dynamic rhythmic turns performed by expert skiers and racers.

So far, we have explored only the highly simplified case where the length of the pendulum leg remains unchanged. As a result, the trajectory of its load is a circular arc symmetric about the vertical direction and hence near the vertical position the load experiences a downward acceleration. In the subcritical regime, this acceleration can be provided solely by the gravitational force. In the supercritical regime, the leg tension is also required when the oscillation amplitude exceeds a certain limit. In this case the pivot is pulled away from the ground. Since skis are not affixed to the snow, they are expected to lift off it in this regime. In fact, in skiing there are occasions when both skis are indeed lifted off the snow. Sometimes this is made intentionally, e.g. during the execution of the so-called "dolphin turn", but more often accidentally, e.g. when skiing over a bump. In ski racing this is generally undesirable due to the inevitable loss of the turning action. Skiers have learned to negate this effect by flexing their legs when going over a real bump or the so-called "virtual bump" in the transition between turns (e.g. LeMaster, 2010, page 40). Hence, we hypothesise that by allowing the pendulum leg to vary in length during its swing we may be able to avoid it being pulled away from the ground at the summit point in the regimes consistent with the practice of alpine racing. The development and investigation of such an advanced model is the main aim of the study described in this paper.

Methods

The basic features of the model are presented in the first paper of the series (Komissarov, 2020). Therefore, here we only briefly describe the common basics and focus on the new developments. A load of mass m is affixed to the upper end of a massless rod of length l whose lower end is attached to a stationary pivot point on a flat horizontal surface. To describe the pendulum motion quantitatively, we use Cartesian coordinates with the origin at the pivot point and the basis vectors $\boldsymbol{i}$, $\boldsymbol{j}$ and $\boldsymbol{k}$ such that the pendulum moves in the plane orthogonal to $\boldsymbol{i}$, and $\boldsymbol{k}$ points upwards in the vertical direction. The position vector $\boldsymbol{r}$ connects the origin with the affixed mass. The inclination angle Ψ is the angle between the vertical direction and the pendulum. We agree that it is positive in the clockwise direction and negative in the anti-clockwise direction.

The load is subject to the vertical gravity force

$$\boldsymbol{F}_g = -mg\boldsymbol{k}\,. \tag{3}$$

the centrifugal force

$$\boldsymbol{F}_c = -(mV^2/R)\,\mathrm{sgn}\,(\Psi)\boldsymbol{j}\,, \tag{4}$$

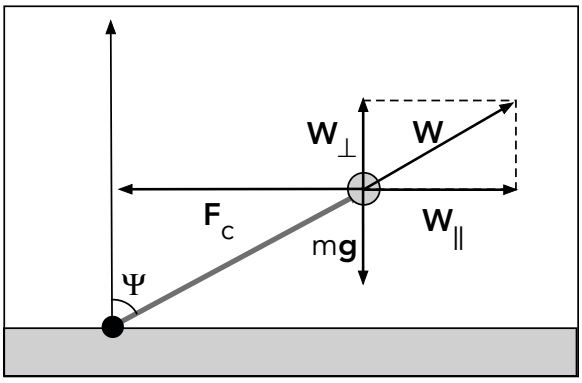

Figure 1. The diagram of forces acting on the pendulum load. $\boldsymbol{F}_c$ is the centrifugal force, $m\boldsymbol{g}$ is the gravity force, and $\boldsymbol{W}$ is the reaction force of the pendulum leg.

where V is the ski speed, R is the curvature radius of the ski trajectory and

$$\operatorname{sgn}\Psi = \begin{cases} +1 & \text{if} \quad \Psi > 0; \\ 0 & \text{if} \quad \Psi = 0; \\ -1 & \text{if} \quad \Psi < 0. \end{cases}$$

is the sign function, and the reaction force of the leg $\boldsymbol{W}$, which ultimately determines the distance between the load and the pivot point, the leg length.

For a perfect carving turn on hard snow

$$R = R_{sc} \cos\Psi \tag{5}$$

(Howe, 1983; Lind & Sanders, 1996). Strictly speaking, this relation is based on the assumption that the penetration of the snow surface by the skis is negligibly small. The values measured by Reid, Haugen, Gilgien, Kipp, and Smith (2020) in a field study of slalom turns performed by elite racers on hard snow are in agreement with equation (5) up to $\Psi = 70°$.

The radial motion of the pendulum mass m is described by the equation

$$ma_r = W + F_{c,r} + F_{g,r}\,, \tag{6}$$

where

$$a_r = \frac{d^2 l}{dt^2} - l\left(\frac{d\Psi}{dt}\right)^2 \tag{7}$$

is its radial acceleration and W is the reaction force of the pendulum leg. In the model we ignore leg's mass, which implies that $W = F_{GR}$, the ground reaction force at the pivot point. When $W < 0$, this is a tension force which resists the action aimed at extending the leg. When $W > 0$, this is a compression force which resists

the action aimed at shortening the leg. In the latter case, W is the effective weight of the load. When measured in the units of mg, the effective weight is called a g-force. In skiing it corresponds to the ground reaction force originated at the skis (Gilgien, Spörri, Kröll, Crivelli, & Müller, 2014).

The swinging motion of the pendulum is governed by the equation

$$\frac{d\boldsymbol{M}}{dt} = \boldsymbol{K}\,, \tag{8}$$

where $\boldsymbol{M} = m\boldsymbol{r}\times\boldsymbol{u}$ is the pendulum angular momentum, $\boldsymbol{K} = \boldsymbol{r}\times\boldsymbol{F}_g + \boldsymbol{r}\times\boldsymbol{F}_c$ is the total torque about the pivot point, and $\boldsymbol{r} = l\sin\Psi\boldsymbol{j} + l\cos\Psi\boldsymbol{k}$ is the position vector (Landau & Lifshitz, 1969). The velocity vector $\boldsymbol{u}$ can be split into the components parallel and perpendicular to the position vector, $\boldsymbol{u} = \boldsymbol{u}_\parallel + \boldsymbol{u}_\perp$, where $\boldsymbol{u}_\perp = l(d\Psi/dt)(\cos\Psi\boldsymbol{j} - \sin\Psi\boldsymbol{k})$. Upon the substitution of all these expressions, equation (8) reduces to

$$\frac{d}{dt}\left(l^2\frac{d\Psi}{dt}\right) = gl\sin\Psi - l\frac{V^2}{R_{sc}}\operatorname{sgn}\Psi\,. \tag{9}$$

Since the leg reaction force $\boldsymbol{W}$ is aligned with $\boldsymbol{r}$, it makes zero contribution to the torque $\boldsymbol{K}$ and effects the swinging motion only via the leg length. Instead of prescribing this force and then solving for the leg length, we may simply prescribe the leg length and then proceed with solving equation (9). The corresponding leg reaction force can be calculated later, via post-processing of the solution, when needed. This is exactly how it is done in the basic model, which assumes l =const.

Here we assume that the pendulum length is a function of the inclination angle and write

$$l(\Psi) = l_0 f(\Psi)\,, \tag{10}$$

where l_0 is its characteristic length scale and $f(\Psi)$ is a differentiable function, which we will refer to as the "retraction function". With this law the pendulum is a closed system and satisfies the energy conservation law (see Appendix A). In what follows, we interpret l_0 as the height of skier's CM from the ground at maximally extended upright position. For the average adult male height of 180 cm (e.g. Roser, Appel, & Ritchie, 2020), and the average ratio between the CM height and the total height of 56% (e.g. Davidovits, 2018, p. 3), l_0 is about one metre. Expert skiers flex their legs in the transition between turns and extend them during the turn (e.g. Harb, 2006; LeMaster, 2010; Reid, 2010). This technique corresponds to $f(0) < 1$.

We further assume that $f(\Psi)$ is a symmetric function, and hence $f(\Psi) = f(-\Psi)$ and $f'(0) = 0$. In application to skiing, this implies that before and after the transition between two turns the extension of skier's legs and the ski tilt angle are related in exactly the same way. Although there is no reason why this should be the case in real skiing, the data provided in Reid (2010) show that this assumption is reasonable. The degree to which skiers extend and flex their legs also varies from turn to turn, as dictated by the terrain and individual preferences. Here we ignore this caveat and focus on the basic effects of the leg action instead.

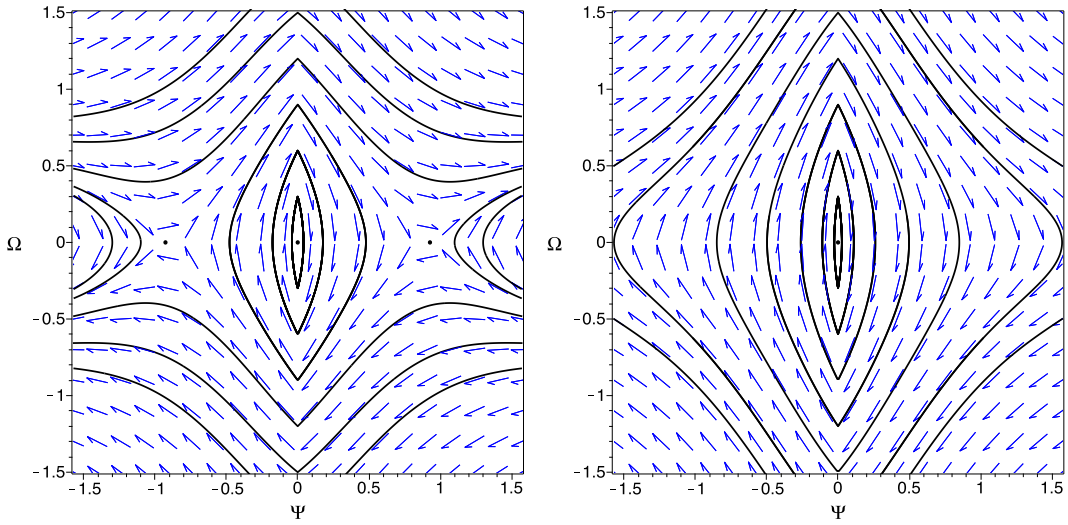

Figure 2. Typical phase portrait of the centrifugal pendulum with a retractable length. The plots correspond to the retraction function of the model B (see section Results for details) with the parameters $b = 0.65$ and $\zeta = 0.8$ (left) and $\zeta = 1.2$ (right). The inclination angle is given in radians.

Via introducing the dimensionless time $\tau = t/T$, where $T = \sqrt{l_0/g}$ is the natural time-scale of the pendulum, equation (9) is reduced to its basic form

$$f(\Psi)\ddot{\Psi} + 2f'(\Psi)\dot{\Psi}^2 = \sin\Psi - \zeta\,\mathrm{sgn}\,\Psi\,, \tag{11}$$

where ζ is the speed parameter given by equation (2), and we use the notations $\dot{A} = dA/d\tau$ and $A' = dA/d\Psi$. The first term on the right side of the equation represents the torque due to gravity, and the second one the torque due to the centrifugal force. The types of solutions allowed by this equation depend on the value of ζ.

To elucidate the properties of a dynamical system described by a second-order ordinary differential equation, it is helpful to convert it into a system of two first-order equations. In our case, the standard conversion yields

$$\begin{aligned} \frac{d\Omega}{d\tau} &= -\frac{2f'(\Psi)}{f(\Psi)}\Omega^2 + \frac{1}{f(\Psi)}(\sin\Psi - \zeta\,\mathrm{sgn}\,\Psi) \\ \frac{d\Psi}{d\tau} &= \Omega\,, \end{aligned} \tag{12}$$

where Ω is the angular velocity of the pendulum. This system allows static solutions (or equilibrium points) which satisfy the condition

$$\frac{d\Omega}{d\tau} = \frac{d\Psi}{d\tau} = 0\,.$$

One of them, $(\Omega, \Psi) = (0, 0)$, describes the vertical position of the pendulum and corresponds to the skier gliding down the fall line. When $\zeta > 1$ (the supercritical

regime) this is the only static solution allowed by the system. When $\zeta < 1$ (the subcritical regime) there are two more static solutions, $(\Omega, \Psi) = (0, \pm \arcsin(\zeta))$, which describe inclined positions on both sides of the vertical and correspond to turns made in perfect balance. Interestingly, these static solutions do not depend on the form of the retraction function $f(\Psi)$. They are exactly the same as in the case of the pendulum with fixed leg length. Hence, phase portraits corresponding to different retraction functions are qualitatively the same if we use the same value of ζ. Figure 2 illustrates the properties of these phase portraits using the retraction function B, described later in Results, as an example. The closed orbits around the origin in the portrait describe pendulum's oscillations about its vertical position – they correspond to the dynamic type of carved turns.

When simulating the trajectories of ski runs based on the pendulum model it is convenient to introduce the length scale $\mathcal{L} = R_{sc}$ and the time scale $\mathcal{T} = R_{sc}/V$. This leads to the dimensionless equations

$$f(\Psi)\frac{d^2\Psi}{ds^2} + 2f'(\Psi)\left(\frac{d\Psi}{ds}\right)^2 = \delta(\zeta^{-1}\sin\Psi - \operatorname{sgn}\Psi)\,, \tag{13}$$

$$\frac{d\gamma}{ds} = \operatorname{sgn}\Psi \sec\Psi\,, \tag{14}$$

$$\frac{d\bar{x}}{ds} = \cos\gamma\,, \tag{15}$$

$$\frac{d\bar{y}}{ds} = \sin\gamma\,, \tag{16}$$

where $s = t/\mathcal{T} = Vt/R_{sc}$, $\bar{x} = x/R_{sc}$, $\bar{y} = y/R_{sc}$, γ is the instantaneous angle of traverse, and the dimensionless parameter $\delta = R_{sc}/l_0$ (Komissarov, 2020). Note that the independent variable s is actually the distance along the trajectory measured in the units of sidecut radius. For simplicity, we will use the initial conditions $\bar{x}(0) = 0$, $\bar{y}(0) = 0$, $\gamma(0) = 0$, $d\Psi/ds(0) = 0$ and $\Psi(0) = \Psi_{max}$. No matter what the dimensional parameters of the problem are, the dimensionless trajectory $\bar{y} = f(\bar{x})$ is completely determined by the initial conditions and the dimensionless parameters ζ and δ.

Results

In the limit of small amplitude ($\Psi \ll \min 1, \zeta$), equation (11) reduces to

$$f(0)\ddot{\Psi} = -\zeta \operatorname{sgn}\Psi\,. \tag{17}$$

This equation has periodic solutions, whose period P depends on their amplitude Ψ_{max}. When $f(0) = 1$ we recover the basic model with non-retractable leg (Komissarov, 2020). Since upon the substitution $\tau = \sqrt{f(0)}\tilde{\tau}$ equation (17) reduces to its

non-retractable form, the period of the retractable solution differs from the period of the non-retractable solution of the same amplitude only by the factor $f^{1/2}(0)$, namely

$$P = 4f^{1/2}(0)\left(\frac{2\Psi_{max}}{\zeta}\right)^{1/2}. \tag{18}$$

Since leg flexion in transition between turns corresponds to $f(0) < 1$, this equation allows us to conclude that such turn technique yields turns that are shorter in duration and, given the same speed, in length compared to the case without flexion.

While the dimensionless period of pendulum oscillations depends only on ζ and Ψ_{max}, the dimensional period also scales like $\sqrt{l_0}$, simply because the employed time scale $T = \sqrt{l_0/g}$. Hence, for the same speed, sidecut radius of skis, and the amplitude of skier's inclination, a shorter skier (with a lower CM) will be making shorter turns compared to a taller skier (with a higher CM). A little bit more information on the scaling with l_0 can be extracted from equations (13)-(16). First, equation (13) shows that $\Psi(s, \delta, \zeta) = F(\delta^{1/2}s, \zeta)$ and hence $s(\Psi, \delta, \zeta) = \delta^{-1/2}S(\Psi, \zeta)$, confirming that the turn length scales like $\sqrt{l_0}$. (Here $F(x, y)$ and $S(x, y)$ are not some specific functions; they are introduced simply to expose the dependence of Ψ and s on δ.) Given this result, equation (14) implies that $\gamma(\Psi, \delta, \zeta) = \delta^{-1/2}\Gamma(\Psi, \zeta)$ and hence

$$\frac{d\bar{x}}{ds} = \cos(\delta^{-1/2}\Gamma(\Psi, \zeta)), \tag{19}$$

$$\frac{d\bar{y}}{ds} = \sin(\delta^{-1/2}\Gamma(\Psi, \zeta)). \tag{20}$$

From this it follows that as l_0 decreases (and hence δ increases), $d\bar{x}/ds$ increases and $d\bar{y}/ds$ decreases and hence the trajectory straightens up even if the range of Ψ and hence the range of the curvature radius R remain the same. Thus, all other things being equal, shorter skiers make not only shorter but also shallower turns.

How skiers flex and extend their legs depends on many factors, including their level and individual preferences. Here we are not aiming at comprehensive analysis and rigorous derivation of general conclusions. Instead, we focus on the most common type of the transition between turns in modern ski racing, which involves legs flexion in transition between turns, and consider in details only two specific examples of the retraction function. These are illustrated in figure 3

Case A

We start with the retraction function

$$f(\Psi) = \frac{a}{\cos\Psi}, \tag{21}$$

which ensures that maximum retraction occurs in the vertical position ($\Psi = 0$), which is the transition point between turns (see the left panel of figure 3). Moreover, in

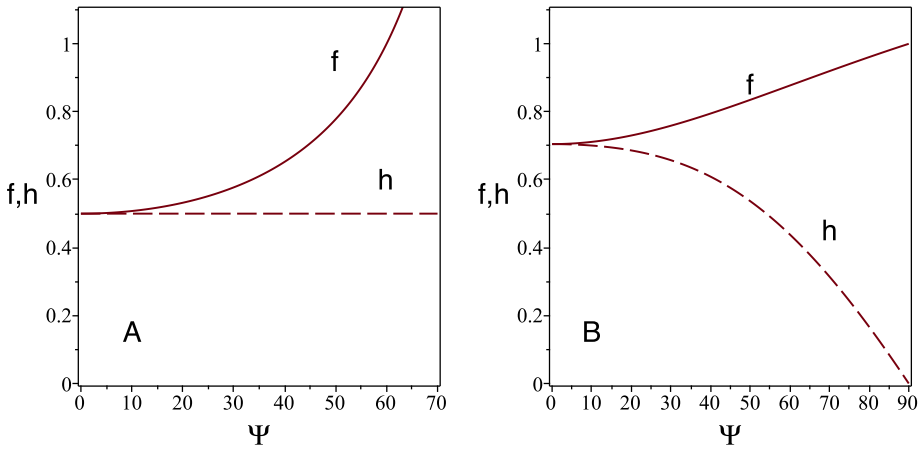

Figure 3. The leg retraction function $f(\Psi)$ and the corresponding height $h(\Psi) = f(\Psi)\cos(\Psi)$ of the pendulum load above the ground in the reference models A (left panel) and B (right panel).

this model the height of the CM above the ground, $H = l_0 f(\Psi)\cos\Psi$, is constant, and hence the vertical acceleration of the CM vanishes completely. Thus, the snow contact is preserved at all time. An excellent video demonstrating this leg action was made available on YouTube by Alltracks Academy (Hetherington, 2016).

Since the full leg extension corresponds to $f = 1$, equation (21) implies the upper limit $\Psi_{lim} = \arccos(a)$ on the inclination angle. Thus, the smaller the value of a is the larger inclination angles can be accommodated. However, in the transition between turns skiers rarely flex their legs beyond the point where the femur bone is parallel to the slope. This is easy to understand as squatting seriously compromises human body's manoeuvrability. When the femur bone is parallel to the slope one may expect a reduction of the CM height by up to a factor of two compared to that in the fully extended upright position, and hence $a = 0.5$. The corresponding maximum inclination angle $\Psi_{lim} \approx 60°$. We are not aware of any study set to determine the lowest position of the CM achievable in the transition between turns of alpine skiing. However, our expectation agrees with the actual measurements taken in the studies of the jump biomechanics (Domire & Challis, 2007). In the rest of the paper, we consider only the case with $a = 0.5$ and refer to it as the model A.

Figure 4 compares the trajectory obtained in model A with the trajectory in the case of fixed leg ($l = l_0$) for the same inclination amplitude. One can see that in the model A the trajectory has a similar curvature but its turns are shorter. The reduction of the turn length is consistent with the reduction of the turn period by the factor $\sqrt{2}$ according to the small-amplitude result (18).

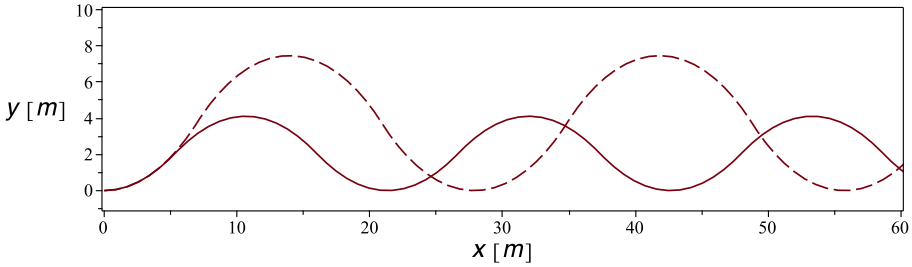

Figure 4. Trajectories of carving runs executed with leg flexion as described in the model A (solid line) and without leg flexion (dashed line; model B with $b = 0$). In both cases $l_0 = 1\,\mathrm{m}$, $R_{sc} = 14\,\mathrm{m}$, $V = 13.7\,\mathrm{m/s}$ ($\zeta = 1.37$) and $\Psi_{max} = 60°$.

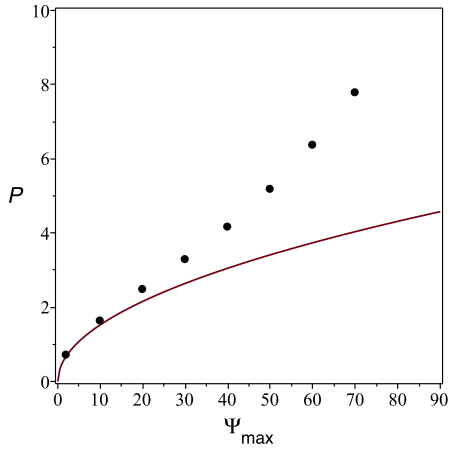

Figure 5. Dimensionless period of the pendulum in the model A with $\zeta = 1.2$. The line shows the period of the small-amplitude solution given by equation (22). The dots show the periods of solutions, which were found via numerical integration of equation (11).

Period-amplitude relation. Since in this model $f(0) = 1/2$, the small-amplitude result (18) reads

$$P = 4\left(\frac{\Psi_{max}}{\zeta}\right)^{1/2}. \tag{22}$$

In the nonlinear regime, the period keeps growing with the amplitude and does this even faster, as this can be seen in figure 5. As a result of this dependence, carving turns with smaller inclination are shorter (see figure 6). They are also straighter because according to Howe's formula smaller Ψ implies smaller curvature of turn's arc. This is similar to what was found in the model with fixed leg length (Komissarov, 2020).

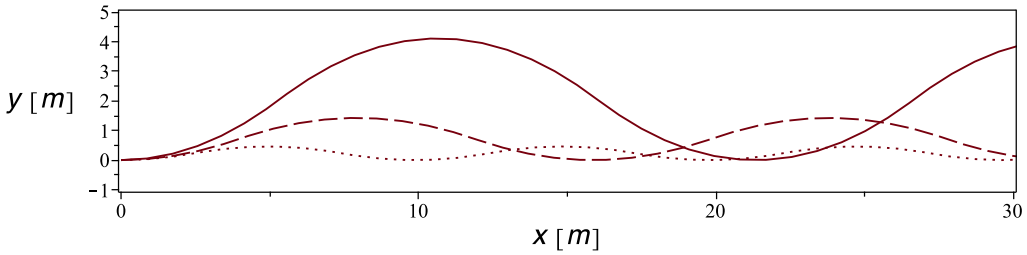

Figure 6. Trajectories of carving run in the model A with for $\Psi_{max} = 60°$ (solid line), $\Psi_{max} = 40°$ (dashed line) and $\Psi_{max} = 20°$ (dotted line). The other parameters are $l_0 = 1\,\mathrm{m}$, $R_{sc} = 14\,\mathrm{m}$ and $V = 13.7\,\mathrm{m/s}$ ($\zeta = 1.37$).

Ground reaction force. In the model A, the leg reaction force is always a compression and the corresponding ground reaction force is

$$F_{GR} = \frac{1}{\cos\Psi}\,. \tag{23}$$

(see Appendix B). Thus, the effective skier's weight does not depend on their speed, contrary to what one would expect given the fact that the centrifugal force, which contributes to the total loading, is speed-dependent. Instead, it is completely determined by the skier inclination.

For the vertical position ($\Psi = 0$), equation (23) yields $F_{GR} = 1$, which is the normal weight of the load. This implies that at transition between carving turns the skis are still loaded quite heavily, making their pivoting problematic. However, in the case of pure carving, skis are simply rolled from edge to edge without pivoting.

At first glance, the lack of dependence of F_{GR} on the speed is a paradox. Indeed, at low speeds the centrifugal force is small and hence F_{GR} must be close to unity, which is not supported by equation (23). However, at low speeds the amplitude of periodic solutions must stay below $\Psi_{eq} = \arcsin(\zeta)$. Because $\Psi_{eq} \to 0$ as $\zeta \to 0$, at low speeds Ψ must be low and hence F_{GR} must be close to unity, as expected. In contrast, for $\zeta > 1$ the inclination angle can have any value between $-\pi/2$ and $\pi/2$, and this indirect dependence of F_{GR} on ζ disappears.

Speed dependence of trajectory. The fact that neither the snow contact condition nor the ground reaction force constrains the skier speed in this model invites us to consider the high ζ regime in some detail. In particular, one may wonder how the skier speed affects the trajectory of their run. Figure 7 shows the results of simulations for slalom skis with $R_{sc} = 14\,\mathrm{m}$ and the speed parameter varying from $\zeta = 1$ to $\zeta = 10$. The inclination amplitude of all these runs is the same, $\Psi_{max} = 60°$. One can see that as ζ increases the turns become shorter and shallower. This could be expected given the form of the right-hand side of equation (13), which increases with ζ, leading to faster variation of the inclination angle with the distance along the trajectory. Figure

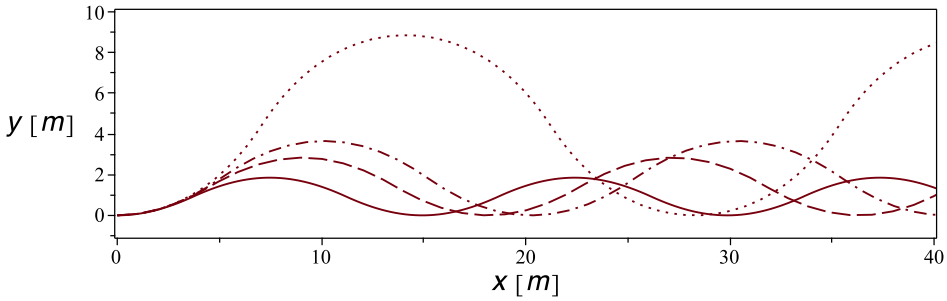

Figure 7. Trajectories in the model A for $\zeta = 1$ (dot line), $\zeta = 1.5$ (dot-dash line), $\zeta = 2$ (dash line) and $\zeta = 10$ (solid line). The other parameters $R_{sc} = 14\,\mathrm{m}$, $l_0 = 1\,\mathrm{m}$ and $\Psi_{max} = 60^\circ$ are the same for all solutions.

7 also suggests that the dependence on ζ weakens as it increases. This is consistent with the fact that as $\zeta \to \infty$ the first term on the right-hand side of equation (13) becomes much smaller compared to the second term and hence the dependence on ζ vanishes. Hence, we should expect the trajectory to approach some asymptotic form. Figure 6 shows that for $\zeta = 10$ the amplitude of the oscillations along the y axis is only just above $l_0 \sin \Psi_{max}$, the horizontal amplitude of the pendulum oscillations in this model. This suggests that the asymptote describes the limiting regime where the skier CM moves straight down the fall line, unaffected by the side-to-side motion of the skis underneath it. However, this has not yet been analytically proved.

Case B

In the case B, we put

$$f(\Psi) = (1 - b\cos\Psi)^{1/3}\,, \tag{24}$$

where b is a parameter. This function has a number of attractive features and this is why it was chosen. Firstly, for the retractability parameter $b = 0$ we recover the pendulum of fixed length. Secondly, it allows a relatively simple expression for the potential energy of the pendulum (see Appendix A). Finally, according to the measurements made by Reid (2010), during a typical SL turn the hight of skier CM reduces from $h \approx 0.7\,\mathrm{m}$ at the transition down to $h \approx 0.4\,\mathrm{m}$ when the ski inclination angle reaches $\Psi_{max} \approx 67^\circ$. The right panel of figure 3 shows the leg retraction function $f(\Psi)$ and the CM-height function $h(\Psi) = f(\Psi)\cos\Psi$ for $b = 0.65$. In this case the CM height h reduces from 0.70 at $\Psi = 0$ to 0.37 at $\Psi = 67^\circ$. Thus, this model introduces the variability of the CM height which is only a little bit more extreme than that measured by Reid (2010). In what follows, we use to the case with $b = 0.65$ as a reference model.

Snow contact condition. Figure 8 compares the ground reaction forces calculated using equation (41) of Appendix B for the case with fixed leg ($b = 0$) and for

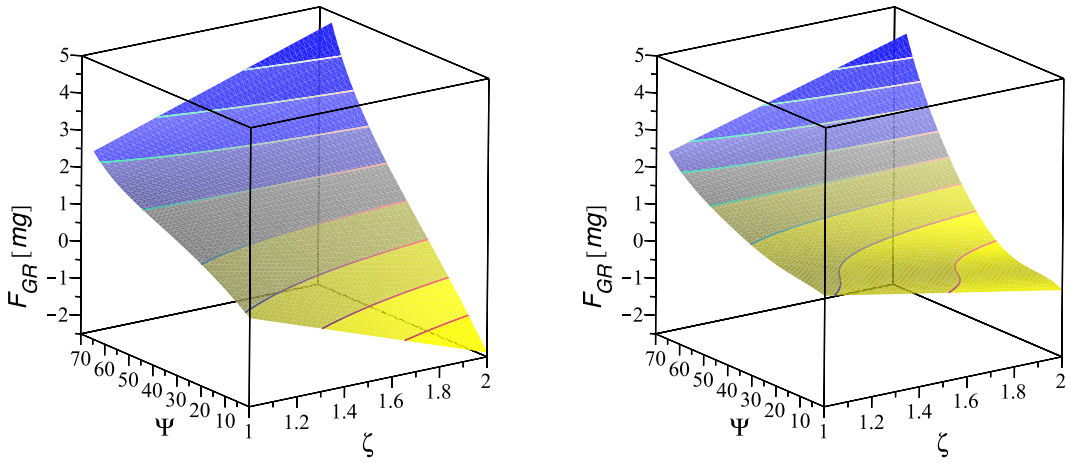

Figure 8. Ground reaction force as a function of ζ and Ψ in the model B with $\Psi_{max} = 65°$. The left panel shows the force in the case of fixed leg ($b = 0$). The right panel shows the force in the case of retractable leg ($b = 0.65$). The force is given in the units of mg.

the case with a retractable leg ($b = 0.65$). In both cases the amplitude of pendulum oscillation $\Psi_{max} = 65°$. Then the force is positive, it is a reaction to the pivot point is pushed into the ground. When it is negative, it is a reaction to the pivot point being pulled away from the ground. Skis can play the role of a pivot only when they are pushed into the snow and we expect them to lift off the snow when the pendulum model predicts $F_{GR} < 0$.

The left panel of figure 8 shows that in the case of fixed leg, $F_{GR} < 0$ near the vertical position ($\Psi = 0$) for nearly all $\zeta > 1$ and becomes very large near $\zeta = 2$. In carving turns describes by such solutions, a skier would be catapulted into the air (cf. Komissarov, 2020). However in the retractable case, the value of F_{GR} near the vertical position is notably higher, and is actually positive for $\zeta < 1.4$. Hence, in this model of the leg action, its flexing at transition also helps to keep skis on the snow. These two scenarios are nicely illustrated by LeMaster (2010) in their Figure 6.3.

Period-amplitude relation. Since in this model $f(0) = (1-b)^{1/3}$, the small-amplitude result (18) reads

$$P = 4(1-b)^{1/6}\left(\frac{2\Psi_{max}}{\zeta}\right)^{1/2}. \tag{25}$$

Hence, the period of the retractable solution is shorter than the period of the non-retractable solution by the factor of $(1-b)^{1/6}$. For the reference model, this is about 16% reduction. The dependence of the period on the amplitude persists in the nonlinear regime. This is illustrated in Figure 9 for the reference model B with

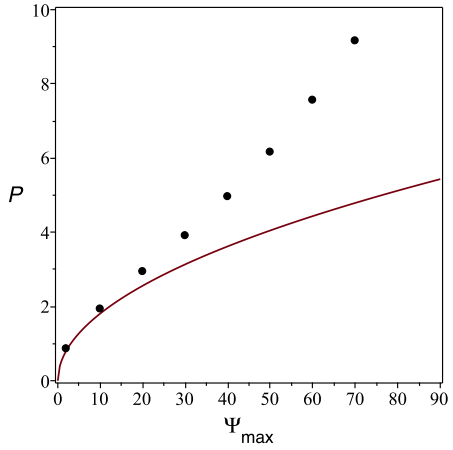

Figure 9. Pendulum period in the reference model B. The line shows the period of the small-amplitude solution given by equation (25). The dots show the period of exact solutions found numerically.

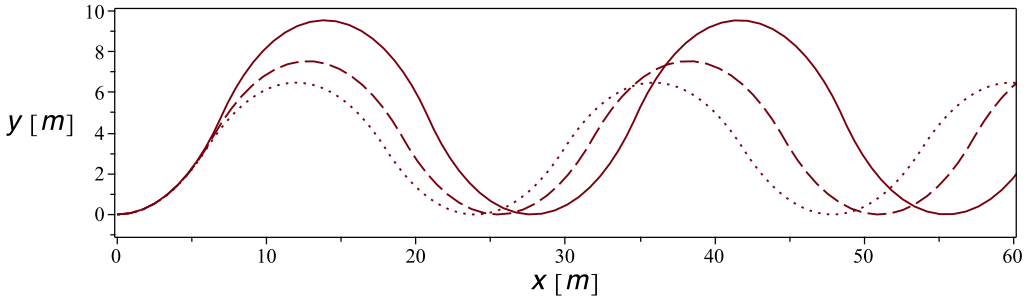

Figure 10. Trajectories of ski runs in the model B with $b = 0$ (solid), $b = 0.6$ (dashed) and $b = 0.8$ (dotted). The other parameters are $l_0 = 1\,\mathrm{m}$, $R_{sc} = 14\,\mathrm{m}$, $V = 13.7\,\mathrm{m/s}$ ($\zeta = 1.37$) and $\Psi_{max} = 65°$.

$\zeta = 1.2$.

The shorter period of solutions with higher retraction parameter b implies shorter carving turns. This is illustrated in Figure 10 where we present the trajectories corresponding to solutions with $b = 0$, 0.6 and 0.8. The other parameters are fixed to $l_0 = 1\,\mathrm{m}$, $R_{sc} = 14\,\mathrm{m}$, $V = 13.7\,\mathrm{m/s}$ and $\Psi_{max} = 65°$. These are chosen to reflect the values measured in the trial runs studied by Reid (2010).

Scaling with the skier height. As we discussed at the beginning of this section, all things being equal, shorter skiers are expected to execute shorter and straighter (shallower) turns, with the turn length scaling as $\sqrt{l_0}$. In order to illustrate the scale of this dependence, we simulated the runs made by skiers of the height 202 cm (Ramon Zenhäusern), 180 cm (Alexis Pinturault), and 165 cm (Albert Popov), thus covering the whole range for current WC slalom racers (figure 11). As one can

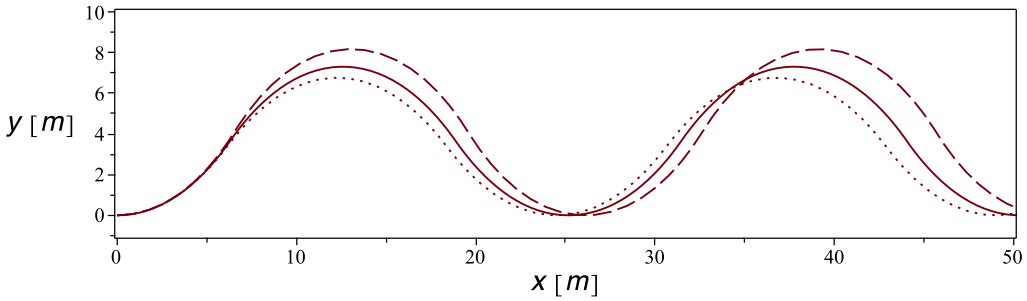

Figure 11. Trajectories of ski runs in the reference corresponding the skier height of 165 cm (dotted line), 180 cm (solid line), and 202 cm (dashed line). The other parameters are $l_0 = 1\,\mathrm{m}$, $R_{sc} = 14\,\mathrm{m}$, $V = 13.7\,\mathrm{m/s}$ ($\zeta = 1.37$) and $\Psi_{max} = 65°$.

see, the difference in the trajectories is not dramatic but appreciable. In order to compensate for this effect, shorter skier would have to go for a higher inclination amplitude and/or higher amplitude of up and down motion (smaller b), making the turn dynamics more extreme.

Peak ground reaction force. The results presented in figure 8 suggest that the peak value of the ground reaction force in the reference model B is not much reduced compared to the case with fixed leg ($b = 0$). In order to check whether this conclusion is specific to $\Psi_{max} = 65°$ or not, we used equation (45) of Appendix B to calculate $F_{GR}^{max} = F_{GR}(\zeta, \Psi_{max})$. This makes sense because the ground reaction force normally peaks at the extreme position of the pendulum, where $\Psi = \Psi_{max}$. In the case with fixed leg, the peak value is given by a relatively simple equation,

$$F_{GR,0}^{max} = \zeta \tan \Psi_{max} + \cos \Psi_{max} \tag{26}$$

(see Appendix B). The left panel of figure 12 shows F_{GR}^{max} for the reference model B, whereas the right panel shows its reduction compared to the model with fixed leg, $\Delta F_{GR}^{max} = F_{GR,0}^{max} - F_{GR}^{max}$. The results confirm that the reduction is indeed rather marginal, and show that for the combination of high ζ and high Ψ_{max} the ground reaction force becomes prohibitive. We compare these values with the actual experimental data in the next section.

Model versus experimental data

With the snow contact issue resolved, it makes sense to carry out a somewhat more detailed check of the pendulum model against the data obtained in experimental studies of turn dynamics in ski racing. This should help to evaluate its current fitness and to identify the ways of further development. In this section, we pay particular attention to the magnitude of the ground reaction force which skiers face during carving turns .

Figure 13 shows the predicted peak value of the ground reaction force as a function of the maximum inclination angle Ψ_{max} and the speed parameter ζ. One

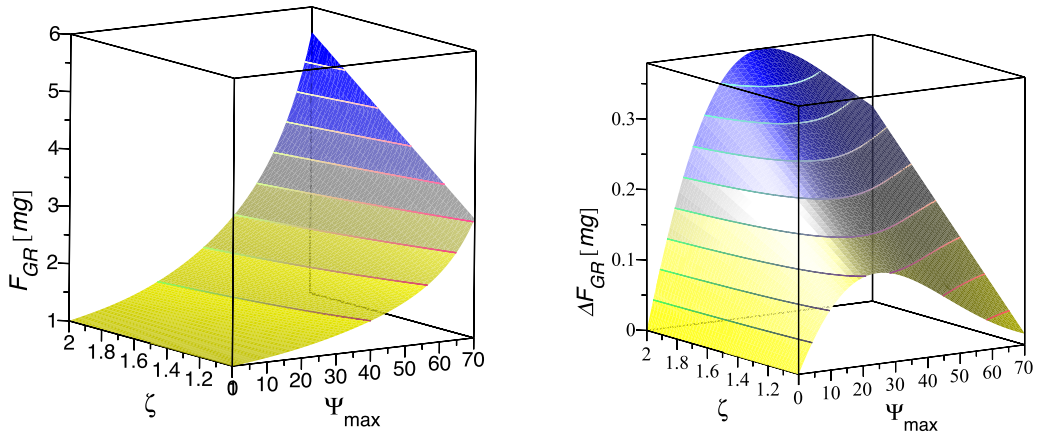

Figure 12. *Left panel:* Peak value of the ground reaction force in the reference model B as a function of the speed parameter ζ and the pendulum amplitude Ψ_{max}. *Right panel:* The reduction of the peak value compared to case with fixed leg. The results are given in the units of mg.

can see that the model A, where the pendulum load remains at the same height throughout its oscillations, yields noticeably lower ground reaction force than the model B, where the load lowers on approach to the turning point.

It is interesting to compare the model predictions with the actual parameters of turns performed by elite athletes. In table 1 we list the maximum speed V_{max}, the shortest local turn radius R_{min} and the peak ground reaction force $F_{GR,max}$ recorded in the field studies of Gilgien et al. (2014) and (Reid, 2010). The data for giant slalom (GS), super-giant slalom (SG) and downhill (DH) are based on the runs made by forerunners of the World Cup competitions during the 2010/11 and 2011/12 seasons (Gilgien et al., 2014). Only the data from the turns with the 10% most extreme values were included in their statistical analysis. It is not possible to say if the peak values of these parameters correspond to the same turn or to different turns. In fact, in ski racing the skier speed is often higher on flatter parts of a race track whereas the turn radius is often smaller on its steeper sections (Gilgien, Crivelli, Spörri, Kröll, & Müller, 2015). The data for GS, SG and DH are simply copied from the table 2 in Gilgien et al. (2014). This paper gives no information on the sidecut radius of skis used in the trials. For this reason, we had to adopt the minimum radius allowed by the FIS regulations for the 2010/2011 season. This should be a reasonably good guess as racers tend to prefer skis with the smallest allowed sidecut radius.

The slalom (SL) data is based on the trial runs made by members of Norwegian national Europa Cup team of the 2005/2006 season. This study used a carefully selected slope which provided uniform conditions throughout a course and courses

Table 1
Parameters of the trail runs studied in Gilgien et al. (2014) and Reid (2010) and the corresponding parameters of the pendulum model. R_{sc} is the assumed ski sidecut radius. $\langle V \rangle$, V_{max}, R_{min}, and $F_{GR,max}$ are, respectively, the mean turn speed, the top speed, the lowest local turn radius, and the top ground reaction force measured during the trials. ζ is the speed parameter of the pendulum model corresponding to $\langle V \rangle$ (for the SL data) or V_{max} (for the GS, SG and DH data) and R_{sc}; Ψ_{max} is the maximum inclination angle corresponding to R_{sc} and R_{min} as prescribed by the Howe formula (Howe, 1983); $F_{GR,A}$ and $F_{GR,B}$ is the ground reaction force in the pendulum model expected for the leg retraction models A and B and given in the units of mg.

Parameter	SL	GS	SG	DH
R_{sc}	14 m	27 m	33 m	45 m
$\langle V \rangle$ or V_{max}	13.7 m/s	22.2 m/s	28.3 m/s	32.3 m/s
R_{min}	6 m	8.4 m	17.2 m	20.6 m
F_{GR}^{max}	3.2	3.16	2.79	2.59
ζ	1.37	1.86	2.47	2.36
Ψ_{max}	65°	71.8°	58.6°	62.7°
$F_{GR,A}^{max}$	2.37	3.20	1.92	2.18
$F_{GR,B}^{max}$	3.23	5.73	4.11	4.62

that promoted repetitive rhythmic skiing with minimal differences between turns. This was done with the aim of accumulating a set of data which was sufficiently large for a robust statistical analysis of the kinematics and dynamics of a typical slalom turn (Reid, 2010). We extracted the data shown in table 1 from figures 6.3, 6.6, 6.10, and 6.32 in Reid (2010) using a basic ruler. Each figure shows the mean value of a displayed parameter and its standard deviation as a function of the turn phase. We used only the mean value curves to determine the turn parameters given in table 1. In particular, $\langle V \rangle$ is defined as an arithmetic mean of the highest and lowest values of the curve for the outside ski speed. R_{min} is the lowest value of the curve for the local turn radius of outside ski, and $F_{GR,max}$ is the highest value of the curve for the ground reaction force. Although these are reached not at exactly the same turn phase, the difference between the phases is not that great. In addition, Reid (2010) presents two separate sets of data, for race courses which had different gate separations. In table 1, we give an arithmetic mean of the numbers found for these two sets. Reid (2010) do not explicitly state the sidecut radius of trial skis but for their calculations they use a model with $R_{sc} = 14\,\mathrm{m}$. So we expect this to be the typical radius of skis in their trials.

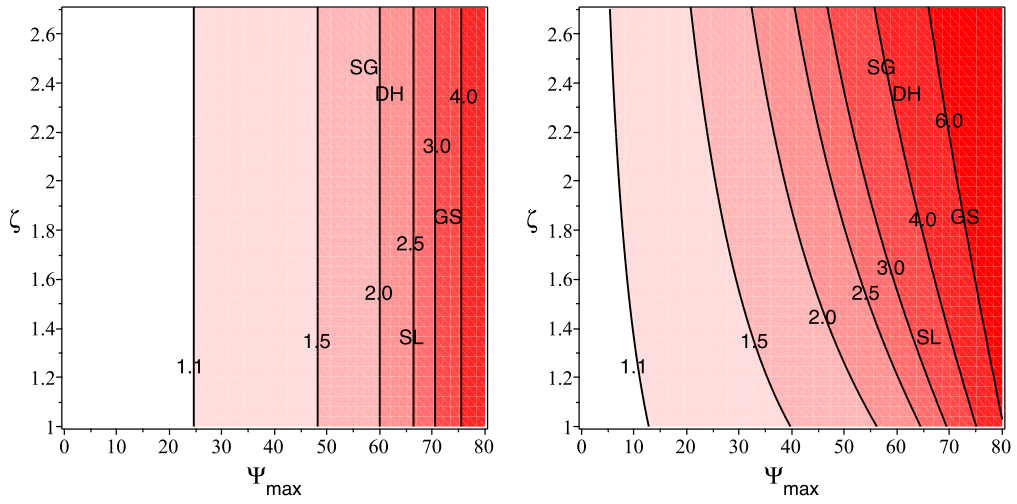

Figure 13. Peak ground reaction force in the reference models A (left panel) and B (right panel) as a function of the speed parameter ζ and the pendulum amplitude Ψ_{max}. We also show the positions corresponding in these models to the peak parameters of the racing runs measured in Gilgien et al. (2014) and Reid (2010).

We use the values of $\langle V \rangle$ (for the SL data) or V_{max} (for the GS, SG, and DH data) and R_{sc} to calculate the values of the speed parameter ζ, using equation (2), and the values of R_{sc} and R_{min} to calculate the ski inclination angle, Ψ_{max}, using equation (5). Finally, the determined values of ζ are fed into equations (45) and (44) to find the corresponding peak values of the snow reaction force expected in the leg retraction models A and B. The results are presented in table 1 and in figure 13.

The most encouraging conclusion that follows from results presented in table 1 is that the peak ground reaction force predicted by the pendulum model for slalom runs using the leg retraction model B is almost identical to the snow reaction force measured in Reid (2010). This is particularly impressive because in this case the model has no free parameters which could be used for fine tuning. Indeed, 1) the retraction model is chosen via fitting the actual variation of the CM height (figure 6.21 in Reid (2010)), 2) the speed parameter ζ is fixed by the measured ski speed and their sidecut radius, 3) the oscillation amplitude Ψ_{max} is fixed by the observed minimum turn radius and the sidecut radius of skis, and 4) there are no other parameters in the model.

For more detailed comparison with the experimental data we have prepared plots showing the evolution of the CM height h, local turn radius R, the ski inclination angle Ψ and the ground reaction force F_{GR} (see figure 14). These are to be compared with figures 6.21, 6.6, 6.10, and 6.32 in Reid (2010) respectively. The data provide two additional quick checks for the model. Firstly, the experimental data give $\Psi_{max} \approx 67°$, which is not far from the theoretical value of $\Psi_{max} = 65°$, indeed. Secondly, the experimental minimum value for the ground reaction force during the transition

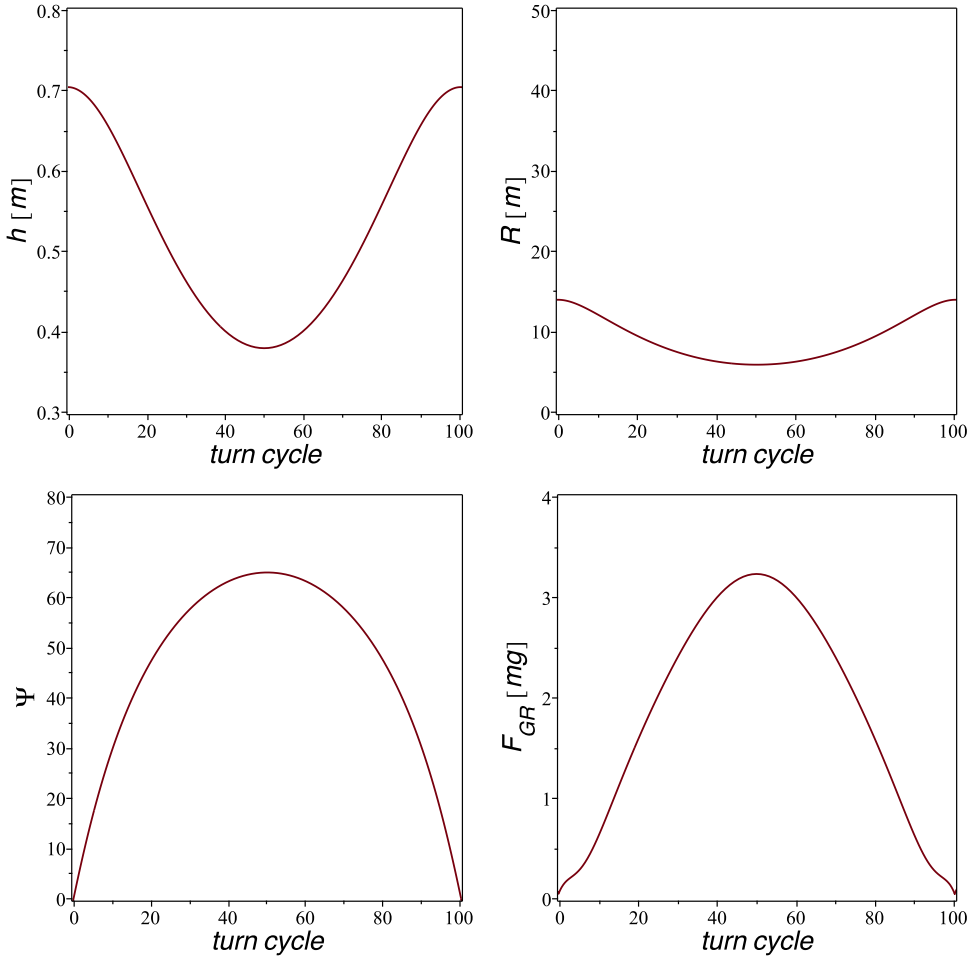

Figure 14. Pendulum CM height above the ground, local turn radius, inclination angle and ground reaction force as a function of the turn cycle (in %) in the reference model B with $l_0 = 1\,\mathrm{m}$, $R_{sc} = 14\,\mathrm{m}$, $\zeta = 1.37$, and $\Psi_{max} = 65°$.

between turns, $F_{GR,min} \approx 0.25\,mg$, which is also similar to what is seen in figure 14. Ignoring the sudden dive at the exact boundary, we find $F_{GR,min} \approx 0.2\,mg$.

The comparison also reveals some notable differences. The most noticeable one is the high local turn radius observed in the experimental data for up to 30% of the turn cycle, in the transition phase. During this period, the turn radius can strongly exceed the ski sidecut radius, implying that skis are not carving. Not only skis but also the skier CM has a much more straightened trajectory during this phase, suggesting an almost inertial motion. This conclusion is supported by a noticeably longer phase of low ground reaction force in the experimental data. In fact, it is common knowledge that skidding and pivoting of skis in transition between turns is an essential part of slalom technique.

Figure 15 shows the ski trajectory predicted in model B using the parameters

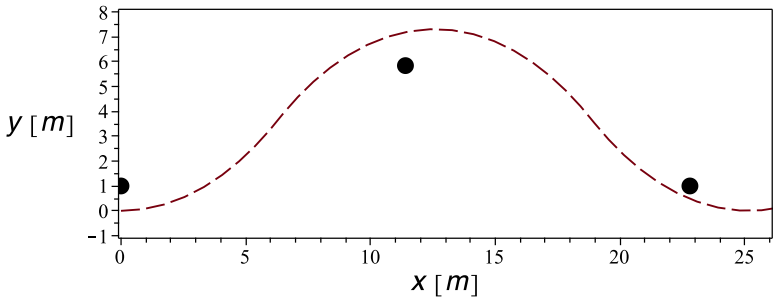

Figure 15. Theoretical ski trajectory predicted in the reference model B versus the gate positioning in Reid (2010). The model parameters are $R_{sc} = 14\,\mathrm{m}$, $l_0 = 1\,\mathrm{m}$, $\zeta = 1.37$ and $\Psi_{max} = 65°$. The distances between turning poles are $\Delta x = 11.4\,\mathrm{m}$ and $\Delta y = 4.84\,\mathrm{m}$.

from table 1 and the position of turning poles as in Reid (2010). Like with other data, we used the arithmetic mean of the distances for the two courses they set. The theoretical turn is a bit longer and wider than needed, with skis clearing the gates with about one metre margin, but given the model simplifications we see this as a reasonable agreement.

As to the results for GS, SG and DH presented in table 1, it is obvious that for all these disciplines, the leg retraction model B predicts peak values of the snow reaction force which significantly exceeds the experimental values and could be unbearable. Moreover, we have found that in all the three cases the model predicts a loss of snow contact in transition between tuns. It could be that V_{max} is measured in one turn and R_{min} in a completely different turn and may be even on a completely different section of the race track. In this case, its possible that in any individual turn the combination of ζ and Ψ_{max} is less extreme, resulting in a lower ground reaction force and a weaker catapulting effect at the end of the turn.

For the model A the predicted peak values of the ground reaction force are closer to the experimental values. In fact, for GS they are almost identical. However, the deduced inclination angle Ψ_{max} exceeds the limiting value $\Psi_{lim} \approx 60°$ of this model. This value of Ψ_{max} corresponds to a 200% increase in the distance between the skier CM and the ski base during the turn, which likely would require skiers to press their knees against their chest at the transition between turns.

For SG and DH the deduced values of Ψ_{max} are approximately equal to Ψ_{lim}, making the model A a more realistic possibility. However, the ground reaction force predicted in this model is significantly below the observed values. This suggests that in the speed disciplines, the height of skier's CM is still variable, but to a lesser extent than in slalom. Although this seems to agree with our naked eye inspection of many openly available video records of WC races, a proper quantitate analysis is required. Overall, the results are not conclusive and more detailed experimental studies of turn kinematics in these disciplines, similar in rigour to Reid (2010), are required for a

more informative analysis.

Since the issue of snow reaction force is important for the prevention of injuries, which trouble the sport, we finish this section by explaining why the model A provides a substantial reduction for the peak values of this force during the turn. At first glance this is rather odd, as for the same speed and the same inclination angle in both models the skier experiences exactly the same centrifugal and gravity forces. However, our simple pendulum model shows that the ground reaction force is also influenced by the leg action, by how fast it is extended and contracted during its swing. This is already evidenced by equations (6) and (7). At the extreme position ($\Psi = \Psi_{max}$), $d\Psi/dt = 0$ and the radial acceleration of the pendulum load reduces to

$$a_r = \frac{d^2 l}{dt^2} \,. \tag{27}$$

As in both models l increases with Ψ, we have $a_r < 0$ at Ψ_{max} and hence the ground reaction force is reduced via the leg action. However, in the model A this effect is stronger. In order to understand why, let us consider all forces acting on the load at $\Psi = \Psi_{max}$. In the model A, the vertical component of the leg reaction force $W_\perp$ must balance the gravity force in order to preserve constant load height above the ground. Hence, $W_\perp = mg$ and the total leg reaction force

$$W = mg(1 + \tan^2 \Psi_{max})^{1/2} \,, \tag{28}$$

just because its vector is aligned with the leg (see figure 1). In the model B, the load height increases after the turning point and hence the vertical component of $\boldsymbol{W}$ must be higher by $\delta W_\perp = m a_\perp$ where $a_\perp$ is the vertical acceleration of the load. For high Ψ_{max}, the corresponding increase of the total reaction force,

$$\delta W = \delta W_\perp (1 + \tan^2 \Psi_{max})^{1/2} \,, \tag{29}$$

can be much higher than $\delta W_\perp$. In the model corresponding to the trial runs in Reid (2010), the total variation of the CM height $\Delta h = 0.33\,\mathrm{m}$. Assuming that for one half of this distance the vertical acceleration is positive, one can estimate its magnitude via the standard equation for the distance covered from rest under constant acceleration,

$$a_\perp = \frac{\Delta h}{T^2} \,, \tag{30}$$

where T is the time required to reach the heigh $\Delta h/2$. This time should be about one-quarter of the whole turn duration. Given the length of the simulated turn $L \approx 14\,\mathrm{m}$ (c.f. figure 15) and the ski speed $V = 13.7\,\mathrm{m/s}$, we estimate $T \approx 0.25\,\mathrm{s}$ and hence $a_\perp \approx 0.5g$, which is not far from the value of $0.37g$ found in our numerical simulations. For $\Psi_{max} = 65^\circ$, this corresponds to $\delta W = 1.12\,mg$, which is not far from the actual difference between the reaction forces in the models A and B (see table 1).

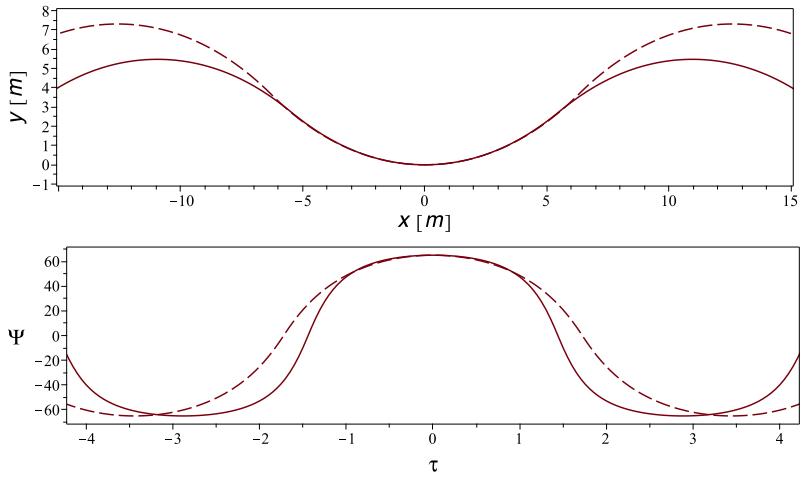

Figure 16. *Top panel:* Ski trajectories in the reference models A (solid line) and B (dashed line) for the same run parameters: $l_0 = 1\,\mathrm{m}$, $R_{sc} = 14\,\mathrm{m}$, $V = 13.7\,\mathrm{m/s}$, and $\psi_{max} = 65°$. *Bottom panel:* The corresponding variation of the inclination angle.

In skiing terms, the model A corresponds to a faster extension of skier's legs (mainly their outside leg) on approach to the turning point and a faster flexion of the legs after passing this point, compared to the model B. The faster flexion means that the skier A offers lesser resistance to the compression coming from the snow. Based on this interpretation, one would expect a smaller impulse received by this skier in the direction normal to the overall direction of travel and hence shallower turns. In figure 16 we compare the ski trajectories in the models A and B for the same parameters as in figure 15. In agreement with our expectation, in the model A the turns are indeed shallower and shorter. Interestingly, the shapes of turn arcs are very much the same in both the cases but the speed of transition from arc to arc is noticeably faster in the model A. This can also be seen in the plots of $\Psi(\tau)$, presented in the lower panel of figure 16.

Discussion and Implications

In this study we aimed to learn more about the potential of the centrifugal pendulum model in capturing essential features of carving turns in expert skiing and racing. The main focus was on how to prevent the loss of snow contact at high speed ($\zeta > 1$) predicted by the basic pendulum model. Indeed, this prediction is in conflict with the skiing practice as $\zeta > 1$ is typical for racing and yet racers manage to avoid being catapulted into the air. The main advice given by ski coaches in this regard is to flex legs in transition between turns and to extend them during turns, the technique analogous to that used in bump skiing for the same reason. Based on this advice, we advanced the pendulum model by allowing variation of its length during oscillations.

The introduction of leg retraction function made the structure of differential

equations governing the pendulum motion a little bit more complex, but a number of its important properties remain unchanged. In particular, it has the same qualitative dependence on the speed parameter ζ. Like in the basic model, for $\zeta < 1$ the pendulum has three equilibrium solutions, and for $\zeta > 1$ these equilibria do no longer exist. This conclusion does not depend on the specific form of the leg retraction function. In application to skiing it means that the leg action does not effect the value of the critical speed above which carving turns become incompatible with lateral balance between the gravity, centrifugal and snow reaction forces.

Like in the basic model (Komissarov, 2020), the period of pendulum oscillations depends on their amplitude, even in the small-amplitude limit, with a smaller amplitude leading to a shorter period. In skiing this implies that reduction of skier inclination during turns results in them becoming shorter and shallower.

Similarly to the basic model, the pendulum period increases with the length of its leg (Komissarov, 2020). In application to skiing this means that, given the same equipment, shorter skiers will tend to make shorter turns compared to taller skiers. To compensate for this, they may be forced to go for more extreme inclination, which increases the turn duration. In agreement with this general period dependence on the pendulum length, we find that contraction of the pendulum leg near the vertical position reduces the oscillation period compared to the case where it remains unchanged (the same as in the extreme position). In skiing this implies that leg flexion in transition between turns makes them shorter, both in duration and in length.

In our numerical modelling, we probed the effect of leg flexion on the snow contact in transition between carving turns using two specific models of this leg action. In our approach we did not aim at building a flexible model which could be used to reproduce the exact action of real skiers, which varies from individual to individual and depends on a number of external factors. Instead, we wanted a relatively simple model which could be easy to implement and analyse.

In the first example (case A) the pendulum load remains at the same height above the ground throughout its oscillation. In skiing this corresponds to such an execution of ski turns that the height of skier's CM above the snow remains invariant throughout a turn. This implies that 1) the vertical component of the leg reaction force applied to the pendulum load always balances the vertical component of gravity force, and 2) the radial component of the ground reaction force at the pivot is always positive. In other words, the pivot is always pushed into the ground. Thus, the setup automatically ensures that the snow contact issue never emerges. We note that in this case, the ground reaction force does not reduce below mg when the pendulum goes through the vertical position. In skiing this implies that such leg action is incompatible with pivoting of skis in transition between turns, which requires skis to be unloaded. However in pure carving such pivoting of skis is completely eliminated, and instead they are simply rolled from one edge to another.

Remarkably, the total ground reaction force corresponding to this leg action does not depend on the speed parameter ζ or the amplitude of pendulum oscillations

Ψ_{max}, but is completely determined by the skis (and hence skier) inclination angle. Moreover, for inclination angles $\Psi < 60^\circ$ the ground reaction force stays rather low, $F_{GR} < 2mg$. At first glance, the lack of dependence on ζ seems to suggest a possibility of turning at extremely high speeds without encountering prohibitively large forces. However as the speed increases, the skier trajectory approaches a straight line, with skis moving from side to side only by the distance dictated by the length of skier's legs and their inclination.

One important limitation of this leg action concerns achievable inclination angles. The model has an upper limit on these angles which is dictated by the lowest anatomically possible heigh of skiers CM above the snow in transition between turns. We estimate this heigh as approximately 50% of the CM height in maximally extended upright position (which is about 100 cm for a 180 cm tall skier). The corresponding limit on the inclination angle is $\Psi_{lim} = 60^\circ$. Although this limit is not low, even more extreme inclinations are often used by top athletes (e.g. see table 1). In addition, skiers do use up and down motion to control the tilt of their skis and hence the turn radius.

In the second example (case B), the pendulum load is allowed to move up and down to a degree controlled by its single parameter b. For $b = 0.65$ the amplitude of this movement is very close to the one observed in slalom turns by (Reid, 2010). In fact, it is noticeably lower than that in the pendulum with fixed leg length, and our calculations show that this has a strong effect on the ground reaction force experienced by the pendulum when it passes its vertical position. For a large section of the parameter space where in the model with fixed leg the pendulum pivot is pulled away from the ground, in the model B it can be still pushed against it. In application to skiing this implies that skis can be kept in snow contact throughout the whole turn cycle. In particular for the parameters of the trial runs described in Reid (2010), the model B predicts $0 < F_{GR} \lesssim 0.25\, mg$, which is in a good agreement with the actual data (Reid, 2010). Since $F_{GR} \ll mg$, the skis are not pressed against the snow as much as in a stationary position and this "unweighting" of skis facilitates their pivoting at transition between turns, which is a typical element of turn technique in slalom.

As to the peak value of the ground reaction force, which is experienced at the extreme pendulum position ($\Psi = \Psi_{max}$), we find that it is only marginally reduced compared to the case with fixed pendulum leg. For the parameters of the trial runs set by Reid (2010), the reference model predicts $F_{GR}^{max} \approx 3.2\, mg$, which is also in a very good agreement with the experimental data. In fact, the reference model B allows to reproduce all basic parameters of the SL runs studied in Reid (2010) quite well. Even the predicted ski trajectory provides a reasonable fitting of their course setting.

Our comparison of the predicted snow reaction force in models A and B shows that the model A allows a substantial reduction of its peak value compared to the model B and suggests that minimisation of the CM heigh variation during skiing turns

can help to reduce the risk of leg injury (cf. Gilgien et al., 2014). The reason behind the difference is due to the additional push against the snow required in the model B in order to initiate the accelerated upward motion of the CM from its lowest position. This additional force increases with the skier inclination angle simply because it has the same inclination and hence must increase in order to support the same vertical acceleration.

We tested the models against the data for GS, SG and DH in Gilgien et al. (2014), who give extreme values of speed, turn radius and snow reaction force encountered in their experiments. Assuming that these apply to a single most extreme turn of their runs, we find that the reference model B overpredicts the peak ground reaction force in speed disciplines, whereas the reference model A underpredicts them. This suggests up and down motion of skiers' CM but to a lesser degree than in slalom. However, more detailed experimental data are needed to reach reliable conclusions.

There is no doubt that the pendulum model is an extremely simplified representation of skiers and their equipment. The human body is much more complex with many degrees of freedom. There is an understandable temptation to build multi-component Hanavan-like models, where both the skier and their equipment are represented by many segments connected by mechanical joints and hope that the power of modern computers will allow to run realistic simulations of skiing (e.g. Oberegger, Kaps, Mössner, Heinrich, & Nachbauer, 2010; Roux, Dietrich, & Doix, 2010). However, in such models one would inevitably face the problem of dealing with highly multi-dimensional phase space. Such problems are computationally very expensive and it is not clear how much can be learned this way. In order to explore the parameter space, it will not be sufficient to run just several simulations. Many more would be needed to allow for optimisation. It will also be difficult to interpret results, to separate key factors from unimportant ones.

The more traditional route of theoretical science is to start from a simple mathematical model including a rather limited number of factors, which are expected to be most important according to current paradigm or practice. Once their role is fully understood, and if the model is found insufficiently realistic, more factors can be included. Our pendulum model is an example of this approach. The good agreement between this model and the experimental studies of slalom turns (Reid, 2010) shows that, in spite of its simplicity, the pendulum model is a useful tool for analysing the dynamics of alpine skiing.

In addition to the leg flexion and extension, there is a number of other aspects of alpine skiing that can be explored using the pendulum model. One aspect which we hope to explore in a foreseeable future is the skier angulation, which makes the ski tilt differ from the CM tilt. This technical element is widely used and considered quite important. For example according to the study by Reid (2010), in slalom turns the CM tilt can be up to 20° smaller than the ski tilt. Such a large difference can have a noticeable effect on the turn dynamics.

Another possible topic is the role of the inside ski/leg. Indeed, in contrast to

the pendulum, skiers have two legs, and in modern skiing they are kept well apart and do not perform as a single unit. In fact, when legs extend during the turn phase, the inside leg extends less compared to the outside one and may even flex (e.g. Harb, 2006; LeMaster, 2010). One may argue that the pendulum leg corresponds to the outside skier leg (the leg which is further away from the centre of turn's arc) because it normally bears most of the load. Since in transition between skiing turns the outside skier leg becomes the inside one and the other way around, for the pendulum with one leg this implies a horizontal shift of its pivot, which can be easily included in the model. A similar shift seems to occur during pivoting of unweighted skis in slalom turns. A next step could be developing a model for a pendulum with two legs.

Conclusion

In this paper we advanced the model of centrifugal pendulum by allowing variation of pendulum length during swinging. This has allowed us to test the hypothesis that such a variation may help to overcome the limitations of the basic model with fixed leg which predicts a loss of snow contact in transition between turns at high speeds characteristic to ski racing. In particular, we have found that leg flexion on approach to the summit point is a very efficient way of preserving the snow contact, in agreement with the practice of ski racing. We have also found that restriction of the up and down motion of skier's centre of mass during turns can allow a substantial reduction of the peak ground reaction force, and hence reduce the risk of injury. Our check of the model against the available data on rhythmic slalom turns made by professional athletes shows a good agreement and allows us to conclude that the model is a very useful tool for deciphering the complicated dynamics of skiing.

Acknowledgments

All non-trivial calculations of this study were carried out with the software package *Maple* (Maple is a trademark of Waterloo Maple Inc.).

Appendix A
Energy of the centrifugal pendulum

It is not very difficult to verify that the Lagrangian of the dynamical system described by equation (11) is

$$L(\dot{\Psi}, \Psi) = \frac{1}{2} f^4 \dot{\Psi}^2 - U(\Psi)\,, \tag{31}$$

where $\dot{\Psi} = d\Psi/d\tau$ and

$$U(\Psi) = -\int f^3(\Psi)(\sin\Psi - \zeta\,\mathrm{sgn}\,(\Psi))d\Psi \tag{32}$$

is the potential energy. The conserved total energy of the pendulum is

$$E = \dot{\Psi}\frac{\partial L}{\partial \dot{\Psi}} - L = \frac{1}{2} f^4(\Psi)\dot{\Psi}^2 + U(\Psi)\,. \tag{33}$$

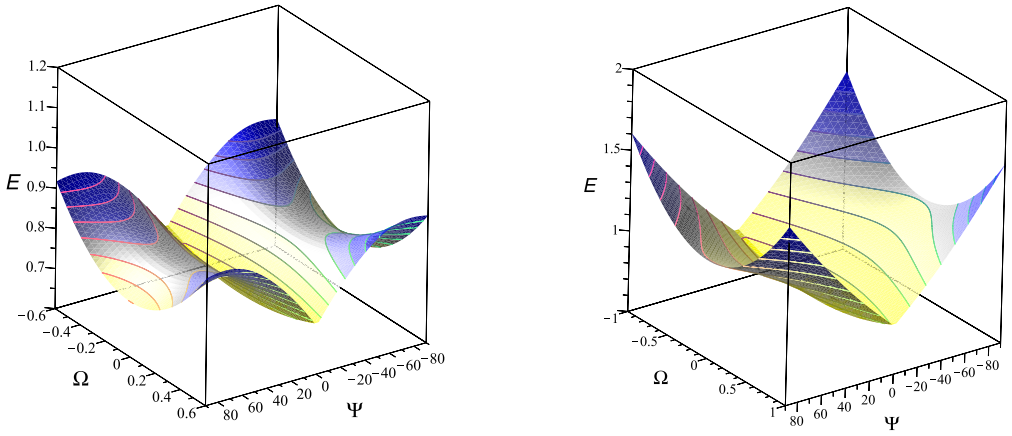

Figure A1. Energy of the pendulum in model B with $b = 0.65$ for $\zeta = 0.8$ (left) and $\zeta = 1.2$ (right).

Since at the turning point $\dot{\Psi} = 0$ and $\Psi = \Psi_{max}$ we have $E = U(\Psi_{max})$.

For $f(\Psi) = (1 - b\cos\Psi)^{1/3}$ equation (32) yields

$$U(\Psi) = -\frac{b}{2}\cos^2\Psi + \cos\Psi + \zeta\left(-b|\sin\Psi| + |\Psi|\right) \tag{34}$$

Figure A1 shows the total energy for $b = 0.65$ and $\zeta = 0.8$, 1.2. In both cases it has a minimum at $(\Psi, \Omega) = (0, 0)$, corresponding the vertical equilibrium of the pendulum. When $\zeta = 0.8$ the function has two saddle points at $(\Psi, \Omega) = (\pm\arcsin(\zeta), 0)$, corresponding to the two inclined equilibria of the system.

For $f(\Psi) = 1/\cos\Psi$ we have

$$16U(\Psi) = -\frac{1}{\cos^2\Psi} + \zeta\,\mathrm{sgn}\,\Psi\left(\sec\Psi\tan\Psi + \ln(\sec\Psi + \tan\Psi)\right). \tag{35}$$

Appendix B
Ground reaction force

The radial motion of the pendulum mass m is described by the equation

$$ma_r = F_{GR} + (\boldsymbol{F}_c + \boldsymbol{F}_g)\cdot\boldsymbol{i}_r\,, \tag{36}$$

where a_r is the radial acceleration, $\boldsymbol{F}_c$ and $\boldsymbol{F}_g$ are the centrifugal and gravity forces respectively (see equations 3 and 4), $\boldsymbol{i}_r = \sin\Psi\boldsymbol{j} + \cos\Psi\boldsymbol{k}$ is the unit vector in the radial direction and W is the ground reaction force at the pivot point. Substituting the expressions for the gravity and centrifugal forces into (36), we find that in the units of mg

$$F_{GR} = \zeta|\tan\Psi| + \cos\Psi + \frac{a_r}{g}\,. \tag{37}$$

The radial acceleration

$$a_r = \frac{d^2 l}{dt^2} - l\left(\frac{d\Psi}{dt}\right)^2 = l_0\left(\frac{d^2 f}{dt^2} - f\left(\frac{df}{dt}\right)^2\right) = g(\ddot{f} - f\dot{f}^2)\,. \tag{38}$$

Since $\dot{f} = f'\dot{\Psi}$ and $\ddot{f} = f''\dot{\Psi}^2 + f'\ddot{\Psi}$, we have

$$\frac{a_r}{g} = (f'' - f)\dot{\Psi}^2 + f'\ddot{\Psi}\,. \tag{39}$$

Using the pendulum equation (11) we find that

$$\ddot{\Psi} = -2\frac{f'(\Psi)}{f(\Psi)}\dot{\Psi}^2 + \frac{\sin(\Psi) - \zeta\,\mathrm{sgn}\,(\Psi)}{f(\Psi)} \tag{40}$$

Substituting this expression into (39) and hence substituting the result into (37), we finally obtain

$$F_{GR} = \zeta|\tan\Psi| + \cos\Psi + \frac{f'}{f}(\sin\Psi - \zeta\,\mathrm{sgn}\,\Psi) + (f'' - \frac{2f'^2}{f} - f)\dot{\Psi}^2\,. \tag{41}$$

Since the energy equation (33) yields

$$\dot{\Psi}^2 = \frac{2}{f^4(\Psi)}(U(\Psi_{max}) - U(\Psi))\,, \tag{42}$$

the ground reaction force is a function of Ψ, its amplitude Ψ_{max}, the speed parameter ζ and whatever parameters enter the expression for the retraction function $f(\Psi)$.

In the case with fixed leg, $f' = f'' = 0$ and (41) reduces to

$$F_{GR,0} = \zeta|\tan\Psi| + \cos\Psi - f\dot{\Psi}^2\,. \tag{43}$$

For $f = 1/\cos\Psi$, the last term in equation (41) vanishes, $f'/f = \tan\Psi$ and hence

$$F_{GR} = \frac{1}{\cos\Psi}\,. \tag{44}$$

In this special case, the ground reaction force does not depend on the speed parameter ζ and the oscillation amplitude Ψ_{max}.

At the turning point $(\Psi, \dot{\Psi}) = (\Psi_{max}, 0)$, and (41) reduces to

$$F_{GR}^{max} = \zeta\tan\Psi_{max} + \cos\Psi_{max} + \frac{f'(\Psi_{max})}{f(\Psi_{max})}(\sin\Psi_{max} - \zeta\Psi_{max})\,. \tag{45}$$

For the case with fixed leg, this equation yields

$$F_{GR,0}^{max} = \zeta\tan\Psi_{max} + \cos\Psi_{max}\,. \tag{46}$$

686 ## References

687 Davidovits, P. (2018). *Physics in biology and medicine*. Cambridge, Massachusetts: Aca-
688 demic Press.

689 Domire, Z., & Challis, J. (2007). The influence of squat depth on maximal vertical jump
690 performance. *Journal of Sports Sciences*, *25*(2), 193-200.

691 Gilgien, M., Crivelli, P., Spörri, J., Kröll, J., & Müller, E. (2015). Characterization of
692 course and terrain and their effect on skier speed in world cup alpine ski racing. *PLoS*
693 *ONE*, *10*, e0118119.

694 Gilgien, M., Spörri, J., Kröll, J., Crivelli, P., & Müller, E. (2014). Mechanics of turning
695 and jumping and skier speed are associated with injury risk in men's world cup alpine
696 skiing: a comparison between the competition disciplines. *British Journal of Sports*
697 *Medicine*, *48*, 742-747.

698 Harb, H. (2006). *Essentials of skiing*. New York: Hatherleigh Press.

699 Hetherington, G. (2016). *Most important move in skiing (part 1): Alltracks academy.*
700 Retrieved from `www.youtube.com/user/AlltracksAcademy/videos`

701 Howe, J. (1983). *Skiing mechanics*. Laporte, Colorado: Poudre Press.

702 Jentschura, U., & Fahrbach, F. (2004). Physics of skiing: The ideal carving equation and
703 its applications. *Canadian Journal of Physics*, *82*, 249-261.

704 Komissarov, S. (2018). *Modelling of carving turns in alpine skiing.* (SportRxiv.
705 https://doi.org/10.31236/osf.io/u4ryc)

706 Komissarov, S. (2020). Dynamics of carving turns in alpine skiing: I: The basic centrifugal
707 pendulum. *Sports Biomechanics*, *25(2)*, 193-200.

708 Landau, L., & Lifshitz, E. (1969). *Mechanics*. Oxford: Pergamon Press.

709 LeMaster, R. (2010). *Ultimate skiing*. Champaign: Human Kinetics.

710 Lind, D., & Sanders, S. (1996). *The physics of skiing: Skiing at the triple point*. New York:
711 Springer-Verlag.

712 Morawski, J. (1973). Control systems approach to a ski-turn analysis. *Journal of Biome-*
713 *chanics*, *6*, 267-279.

714 Oberegger, U., Kaps, P., Mössner, M., Heinrich, D., & Nachbauer, W. (2010). Simulation
715 of turns with a 3d skier model. *Procedia EnginFeering*, *2(2)*, 3171-3177.

716 Reid, R. (2010). *A kinematic and kinetic study of alpine skiing technique in*
717 *slalom* (PhD dissertation, Norwegian School of Sport Sciences). Retrieved from
718 `http://hdl.handle.net/11250/171325`

719 Reid, R. C., Haugen, P., Gilgien, M., Kipp, R. W., & Smith, G. A. (2020). Alpine ski
720 motion characteristics in slalom. *Frontiers in Sports and Active Living*, *2*, 25-36.

721 Roser, M., Appel, C., & Ritchie, H. (2020). "human height". *"Our World in Data"*. Retrieved
722 from `https://ourworldindata.org/human-height`

723 Roux, F., Dietrich, G., & Doix, A.-C. (2010). Skier-ski system model and de-
724 velopment of a computer simulation aiming to improve skier's performance and
725 ski. In *Proceedings of the 1st augmented human international conference* (p. 13).
726 New York, NY, USA: Association for Computing Machinery. Retrieved from
727 `https://doi.org/10.1145/1785455.1785468`